Tellus (1999), 51B, 919–937
Printed in UK. All rights reserved

TELLUS
ISSN 0280–6509

Modelling the production and cycling of dimethylsulphide during the vernal bloom in the Barents Sea

By ALBERT J. GABRIC[1]*, PATRICIA A. MATRAI[2] and MARÍA VERNET[3], [1]*School of Australian Environmental Studies, Griffith University, Nathan, Queensland, Australia;* [2]*Bigelow Laboratory for Ocean Sciences, 180 McKown Point, West Boothbay Harbor, Maine 04575-475, USA;* [3]*Marine Research Division, Scripps Institution of Oceanography, La Jolla, California 92093-218, USA*

(Manuscript received 23 December 1998; in final form 31 May 1999)

ABSTRACT

Recent field work suggests an important rôle for the Arctic Ocean in the global budget of dimethylsulphide (DMS), a climatically active volatile sulphur compound. Here, we have used an existing DMS production model and local field data to examine the temporal dynamics of the DMS cycle during the spring bloom in the Arctic shelf of the Barents Sea. The timing and duration of the spring phytoplankton bloom has been shown to be a key determinant of the flux of DMS to the atmosphere. Particular oceanic conditions due to the retreating ice-edge (e.g., a shallow mixed layer) can have an important effect on the timing of the phytoplankton bloom and thus the efflux of DMS in this region. Model simulations support the view that algal taxonomy is not the most important factor determining DMS production in these waters. The mean vernal DMS flux is predicted to be 0.063 mg S m^{-2} d^{-1} which is in general agreement with previous summer season averages in the Arctic.

1. Introduction

Dimethylsulphide (DMS) is a volatile sulphur compound produced in oceanic surface waters by certain classes of marine phytoplankton (Keller et al., 1989). Oceanic DMS concentrations are high enough to sustain a net flux to the atmosphere, currently estimated to be 0.5 ± 0.3 T mol S yr^{-1} (Bates et al., 1992) which may influence global climate (Charlson et al., 1987; Shaw, 1987; Meszaros, 1988). Once ventilated to the atmosphere, DMS is oxidised to form non-sea-salt sulphate and methanesulphonate (MSA) aerosols which can exert a cooling effect on climate both directly (by scattering incoming solar radiation) and indirectly (by increasing cloud albedo).

The production of DMS and its precursor β-dimethylsulfoniopropionate (DMSP) in the polar oceans seems to be particularly enhanced (Gibson et al., 1990; McTaggart and Burton, 1992; Matrai and Vernet, 1997) suggesting that these regions contribute significantly to the global atmospheric sulphur burden. In sub-Arctic, Arctic, and Antarctic waters, the presence of *Phaeocystis* sp., strong DMS producers, is thought to influence the elevated concentrations of DMS observed (Barnard et al., 1984; Liss et al., 1994; Matrai and Vernet, 1997). Arctic concentrations of MSA exhibit strong seasonal variability and it has been suggested that this is due to a seasonal cycle in DMS emissions (Li et al., 1993; Heintzenberg and Leck, 1994). Ice algae have also been shown to be significant producers of DMS and DMSP in both Antarctic and Arctic regions (Kirst et al., 1991; Levasseur et al., 1994).

Recently Matrai and Vernet (1997), hereafter referred to as Paper I, reported the first compre-

* Corresponding author.
E-mail: a.gabric@mailbox.gu.edu.au

hensive study of DMS and DMSP cycling in the Barents Sea. Surprisingly, they found that diatoms contributed as much as prymnesiophytes (which are considered high DMSP producers) to the water column budgets of DMSP and DMS. The physiological stage of the bloom appeared to be the main factor controlling DMS production rather than taxonomic composition. Cycling of DMS in the surface layer was thought to be mainly due to microbial consumption in ice-free waters, although in polar front waters microbial activity was depressed and ventilation to the atmosphere was the dominant sink.

Here we present a modelling analysis of the production and cycling of DMS in the Barents Sea with the aim of quantifying the production of DMS during the vernal bloom and estimating the flux of DMS to the atmosphere in this area. The field data of Paper I were collected over a short time period at each station and thus provide a "snap-shot" of the bloom dynamics and sulphur budget. Significantly, the field data have allowed the accurate specification of many of the model parameters which were previously poorly defined. Of the 34 model parameters, only 16 were taken from the general literature, with 18 derived from either the field data collected in Paper I or from contemporaneous studies conducted in the Barents Sea by other workers. This means the uncertainty in the model predictions has been significantly reduced compared with generic (non-site-specific) studies published previously.

The modelling analysis enables temporal extrapolation of the limited data and are important for our understanding of the dynamics of Arctic sulphur cycling where, due to the extreme conditions, data-sets will probably always be sparse. The model allows a more accurate estimate of seasonal emissions of DMS to the atmosphere and highlights the significant rôle of the Arctic region on global climate change.

2. Characteristics of the study site

As discussed in Paper I, the Central Barents Sea was sampled during May 1993 along a transect from 76°32′N, 32°55′E to 72°45′N, 30°21′E (Fig. 1). Process studies were done at four stations, (Station I, 76.5°N to Station IV, 73.5°N), which were chosen to sample the varied oceanic conditions (i.e., percent ice-cover and phytoplankton community composition) encountered along the transect. A summary of the physical conditions at each of the stations is given in Table 1 and a complete description of the physical conditions in the Barents Sea can be found in Loeng (1991) and Wassmann et al. (1998).

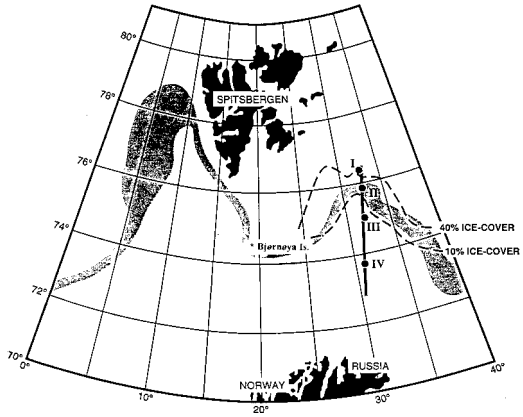

Fig. 1. Map of western Barents Sea with cruise transect (solid line) and sampling stations (circles). The polar front in the ocean is shaded.

During spring and summer the waters at the ice-edge (defined as 40% ice coverage) are characterised by high primary production (1 to 3 gC m^{-2} d^{-1}) and a bloom of long duration, as the ice gradually recedes northward (Rey, 1991; Wassmann et al., 1990). Diatoms (mainly *Chaetoceros* and *Thalassiosira* sp.) and prymnesiophytes (*Phaeocystis* sp.) dominate the phytoplankton community. Diatoms were the major community component at Stations I and IV with a mixture of diatoms and prymnesiophytes present at Stations II and III. A previous studies in this area found that nitrate is the dominant nitrogen source for phytoplankton growth during the pre- and post bloom periods which concern us here (Kristiansen et al., 1994).

Along the transect, surface chlorophyll *a* concentration varied from 1.5 μg chl l^{-1} in ice-free waters to 6 μg chl l^{-1} in the marginal ice zone and reached a maximum value of 13.5 μl chl l^{-1} under the ice. Nutrient concentrations decreased northward with the lowest values measured in ice-covered waters (at Station I). The field data collected during May 1993 suggest that the bloom

Table 1. *Oceanic conditions at each of the stations*

	Station I	Station II	Station III	Station IV
location	76°22.9′N	75°49.2′N	74°59.2′N	73°44.1′N
date sampled (Julian Day)	138–40	141–2	143–4	145–6
water mass	Arctic	polar front	Atlantic	Atlantic
mixed-layer temp. (C)	−1.6	0.8	2.7	3.6
mixed-layer salinity (‰)	34.37	34.49	34.99	34.94
euphotic depth*, Z_e (m)	15	26	35	38
mixed-layer depth, MLD (m)	36	14	65	61
$R = \mathrm{MLD}/Z_e$	2.4	0.54	1.9	1.6
winter NO_3 (μM)	11	11	11	11
ice-cover (%)	55	40	10	0
annual temp. range (°C)	−1.5–0.0	−0.5–2.0	2.5–6.5	2.5–6.5

* Defined as the 1% surface irradiance level.

developed first in the north under melting ice and later in Atlantic waters (Vernet et al., 1998).

Particulate organic sulphur (POS) tracked the chlorophyll *a* gradient along the transect with the highest concentrations measured in Atlantic ice-covered waters. Mean surface DMS concentrations were high along the transect increasing from about 5.5 nM in ice-free waters to 16.5 nM at the polar front. Mean surface DMSP concentrations were 8.6 nM in the dissolved phase and 16.5 nM in the particulate phase and followed a similar gradient to POS and chlorophyll *a* along the transect. By comparison, Bates et al. (1987) reported mean summer DMS concentrations of around 1.5 nM for ice-free waters in the Pacific in a latitude band 65–73°N. Leck and Persson (1996) have reported DMS concentrations in the range 5–18 nM during July in the Barents Sea.

3. Model structure and parameter estimation

The DMS production model was originally described in Gabric et al. (1993) and an extended version including seasonal light and temperature variation and a detailed formulation of the DMS sea-to-air transfer velocity has been applied to the Subantarctic Southern Ocean (Gabric et al., 1995, 1996, 1998). Here we discuss the adaptation of the model to the conditions pertaining to the Barents Sea.

The model food web reflects the current ecological paradigm with micro-organisms playing a central rôle in elemental recycling (Azam et al., 1983; Fenchel, 1988) and also influencing DMSP and DMS turnover in the water column (Kiene and Bates, 1990). The model is time-dependent with state variables vertically averaged over the oceanic mixed layer, which is assumed to be of constant depth during the period of simulation.

The biotic state variables include a generic phytoplankton, planktonic bacteria which metabolise DMS and DMSP, and three heterotrophs: bacterivorous nanoflagellates, large protozoa (e.g., ciliates), and macrozooplankton. For simplicity, no higher trophic levels are considered although zooplankton export through grazing by fish has been included. Abiotic state variables include dissolved inorganic nitrogen, DMSP and DMS. The model uses dual elemental currencies of nitrogen and sulphur with conversion between carbon and nitrogen done using a C : N ratio (by weight) of 6.0 for phytoplankton and 5.0 for bacteria (Strickland, 1960; Nagata, 1986). C : Chl *a* ratios were taken to be as previously measured for the process study areas in the Barents Sea by Rey (1991). The model food web shown in Fig. 2 is conceptually similar to that most recently described for Arctic waters by Nielsen and Hansen (1995), except these authors subdivided the phytoplankton into two size classes. The model state variables and observed values for each station are listed in Table 2. The fluxes between state variables are as described in Gabric et al. (1993).

3.1. Phytoplankton growth

Phytoplankton growth in the mixed layer is assumed to depend on nutrient concentration, vertically-averaged irradiance, and sea temper-

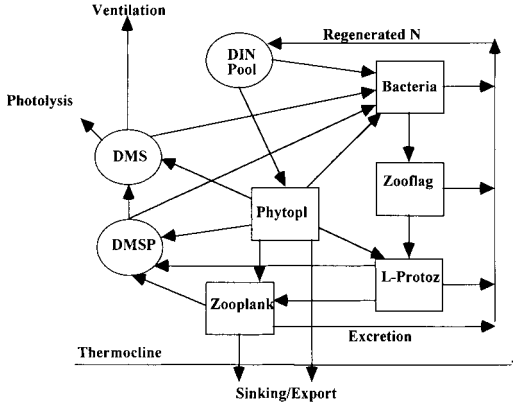

Fig. 2. Model food web structure. Fluxes shown with arrows indicating flow of N or S (see Table 3).

ature — the so-called multiplicative growth model (Platt et al., 1977). The specific nutrient uptake rate at time t is given by,

$$\mu(t) = V_N(t)R_L(t)R_T(t), \quad (1)$$

where V_N (h^{-1}) is the maximum nitrate-specific uptake rate following standard Michaelis–Menten kinetics, and R_L and R_T are dimensionless light and temperature limitation coefficients, respectively, both $\leqslant 1$. Nitrogen, as ammonium is regenerated via heterotrophic excretion in the food web, however, the model formulation does not distinguish between nitrate and ammonium uptake. This simplification does not introduce a significant error as observations in the Barents Sea (Kristiansen et al., 1994) indicate that "new" production is very high (92–96%) during the pre-bloom and bloom periods which concern us here.

Although the model food web treats phytoplankton as a homogeneous group, taxonomic differences between phytoplankton at each station are reflected in the values of the relevant phytoplankton model parameters, including V_N (h^{-1}) the maximum nitrate-specific uptake rate. DMSP production can also be affected by algal taxonomy and this is included by the definition of the model parameter γ, the mean cell S:N ratio, which reflects the algal DMSP content (Table 3).

Photosynthetically active radiation (PAR) at the sea-surface was calculated using a radiation model (Brock, 1981), which was calibrated using in situ irradiance measurements taken along the transect by Matrai and Vernet (1997). Mixed layer average irradiance was computed by assuming the Beer–Lambert law for water column extinction with the extinction coefficient derived from in situ measurements of euphotic zone depth (assumed to be where irradiance is reduced to 1% of the surface value). Light limitation of phytoplankton growth has been modelled following Smith (1936) as,

$$R_L = P/P_{max} = (I/I_k)(1 + (I/I_k)^2)^{-0.5}, \quad (2)$$

where P is the gross photosynthetic rate, P_{max} the maximum photosynthetic rate, I the irradiance at a particular depth, and I_k the saturating irradiance (Talling, 1957) which was measured from incubation experiments at each station. We have chosen this model as it involves a single parameter I_k that was measured at the each of the stations (Table 4). The average light limitation may be computed by integrating R_L over the mixed layer depth, however a very good approximation is obtained by substituting the vertically averaged irradiance for I in eq. (2).

The effect of temperature on the growth rate of phytoplankton was based on the formulation

Table 2. *Observed values of state variables (mixed layer means) for Stations I–IV*

State variable	Definition (units)	St I	St II	St III	St IV
P	generic phytoplankter (mg N m^{-2})	4031	285	605	985
B	planktonic bacteria (mg N m^{-2})	486.6	131.2	170.3	412.1
F	bacterivorous nanoflagellates (mg N m^{-2})	8.7	29.4	16.6	12.6
LP	large protozoa (mg N m^{-2})	67.5	5.2	2.43	45.8
Z	micro/mesozooplankton (mg N m^{-2})	185.5	49.6	80.7	131.9
N	dissolved inorganic N (mg N m^{-2})	1701	878	7042	5110
DMSP	dissolved DMSP (mg S(DMSP) m^{-2})	16.0	11.6	33.2	24.9
DMS	dissolved DMS (mg S(DMS) m^{-2})	14.9	2.8	9.9	9.7

Table 3. *Definition of model fluxes (k parameters are defined in Table 4)*

Code	Formulation	Meaning
F12	k1*B*P/[P + k2]	bacterial decomposition of detrital phytoplankton(P)
F14	k3*P*LP	grazing of P by large protozoa (LP)
F15	k4*P*Z	grazing of P by zooplankton (Z)
F17	k5*γ*P	release of DMSP by P
F18	γ*k6*P	release of DMS by P
F1W	k7*P	sedimentation of P below thermocline
F23	k8*F*B/[B + log(2)/k9]	grazing on bacteria (B) by zooflagellates (F)
F26	k10*B + k11*[F62 + F12]	regeneration of dissolved nitrogen by B
F34	k3*F*LP	grazing on F by LP
F36	k13*F + k14*F23	regeneration of dissolved N by F
F46	k16*LP + k17*[F34 + F14]	excretion of dissolved N by LP
F47	γ*k18*LP	excretion of DMSP by LP
F56	k19*Z + k20*[F15 + F45]	excretion of dissolved N by Z
F5w	k22*F56 + K32*Z	sedimentation and export of Z to higher trophic levels
F61	R_L*R_T*k23*P*N/[N + k24]	uptake of dissolved N by P (see eqs. 1–3)
F62	k25*B*N/[N + k26]	uptake of dissolved N by B
F72	k31*DMSP	biodegradation of DMSP by B
F78	k27*DMSP	conversion of DMSP to DMS in water column
F82	k28*DMS	biodegradation of DMS by B
F8w	k29*DMS	photo-oxidation and other sinks for DMS
F8a	K_w*DMS	ventilation of DMS to atmosphere

given by Eppley (1972),

$$R_T = \exp(0.063(T - T_{max})), \quad (3)$$

where T is the mean mixed layer temperature (°C), and T_{max} the maximum temperature achieved during the bloom period (Table 1). Mixed layer temperature during the bloom period is calculated following Gabric et al. (1998), namely, by a sinusoidal function with a period of a year and amplitude given by the temperature range quoted for each of the three water masses in Table 1.

It should be noted that the data-set used by Eppley (1972) excluded temperatures below zero, which are encountered in the Barents Sea. There is some evidence that phytoplankton growth is suppressed at low temperatures (Bunt and Lee, 1970; Pomeroy and Diebel, 1986). However, investigations on temperature limitation by Slagstad and Støle-Hansen (1991) in the Barents Sea and Neori and Holm-Hansen (1982) in Antarctic waters support the formulation used here.

3.2. *Bacterial growth*

Two conflicting views exist on the rôle of bacteria in the Arctic marine food-web. Studies in Newfoundland coastal waters (Pomeroy and Diebel, 1986) reported inhibition of bacterial production at low temperatures or due to substrate limitation. However other data collected in the Barents Sea (Thingstad and Martinussen, 1991), the Bering Sea (Andersen, 1988) and the central Arctic (Rich et al., 1997) suggest that bacterial activity may be comparable to that found in temperate waters.

Rivkin et al. (1996) reviewed microbial activity in permanently cold $T < 4$°C, seasonally cold $T < 4$°C, and temperate environments $T > 4$°C for temperature-growth relationships. Significant correlation between specific growth rate and temperature was found only for $T > 4$°C. The mean specific growth rate for cold waters (average temperature of -0.8°C) was 0.39 ± 0.42 d^{-1} (range: 0.0002–2.1 d^{-1}). Muller-Niklas and Herndl (1996) reported a similar value for average bacterial growth rate in the Barents Sea of 0.31 ± 0.10 d^{-1} (range: 0.21–0.53 d^{-1}), at an average temperature of -0.7°C. Recent measurements by Rich et al. (1997) and Sherr et al. (1997) in the central Arctic also support this range. In contrast, Nielsen and Hansen (1995), who studied carbon cycling during June–July at a site off western Greenland, reported lower values of bacterial specific growth rate in

Table 4. *Definition and values of model parameters: Stations I-IV*

	Pathway (units)	St I	St II	St III	St IV	Ref†
k1	max. uptake rate of detrital N by B (d^{-1})	0.31	0.31	0.31	0.31	(1)
k2	half-saturation conc. for B uptake of detrital N (mg N m^{-2})	693.1	288.8	1307.8	1155.2	(8)
k3	LP grazing rate per organism (m^2 mg N^{-1} d^{-1})	0.5e–3*	1.2e–3	1.2e–3	0.5e–3	(5)
k4	*Z* grazing rate per organism (m^2 mg N^{-1} d^{-1})	0.5e–3*	1.2e–3	1.2e–3	0.5e–3	(5)
k5	release rate of DMSP by P (d^{-1})	0.01	0.01	0.01	0.01	(3)
k6	release rate of DMS by P (d^{-1})	0.0085	0.0085	0.0085	0.0085	(3)
k7	P-cell sinking rate (d^{-1})	0.020	0.27	0.12	0.004	(2)
k8	max. uptake rate of B by F (d^{-1})	1.67	0.89	0.63	1.25	(5)
k9	half-saturation conc of B by F (mg N m^{-2})	182.4	70.7	330.1	301.4	(3)
k10	B specific excretion rate (d^{-1})	0.07	0.07	0.07	0.07	(3)
k11	proportion of N uptake excreted by B	0.63	0.63	0.63	0.63	(3)
k12	grazing rate of F by LP per organism (m^2 mg N^{-1} d^{-1}) (assumed = k3)	0.5e–3*	1.2e–3	1.2e–3	1.2e–3	(5)
k13	F specific excretion rate (d^{-1})	0.05	0.05	0.05	0.05	(3)
k14	proportion of N uptake excreted by F	0.65	0.65	0.65	0.65	(3)
k15	grazing rate of LP by Z per organism (m^2 mg N^{-1} d^{-1}) (assumed = k4)	0.5e–3*	1.2e–3	1.2e–3	1.2e–3	(5)
k16	LP specific N excretion rate (d^{-1})	0.05	0.05	0.05	0.05	(3)
k17	proportion of N uptake excreted by LP	0.65	0.65	0.65	0.65	(3)
k18	DMSP excretion rate by LP (d^{-1})	0.01	0.01	0.01	0.01	(3)
k19	Z specific N excretion rate (d^{-1})	0.05	0.05	0.05	0.05	(3)
k20	proportion of N uptake excreted by Z	0.4	0.4	0.4	0.4	(3)
k21	DMSP excretion rate by Z (d^{-1})	0.01	0.01	0.01	0.01	(3)
k22	*Z* sinking rate (d^{-1})	0.020	0.36	0.14	0.035	(2)
k23	max. N uptake rate by P (d^{-1})	0.27*	0.4	0.55	0.25*	(6)
k24	half-saturation conc. for N uptake by P (mg N m^{-2})	252.1	97.6	462.1	433.2	(7)
k25	max. N uptake rate by B (d^{-1})	0.31	0.31	0.31	0.31	(1)
k26	half-saturation conc. for N uptake by B (mg N m^{-2})	69.3	28.9	130.8	115.5	(8)
k27	DMSP-DMS conversion rate (d^{-1})	0.5	0.5	0.5	0.5	(3)
k28	DMS consumption rate by B (d^{-1})	0.29	0.18	0.52	0.35	(2)
k29	max. DMS photo-oxidation rate (d^{-1})	1.3	1.3	1.3	1.3	(4)
k31	DMSP consumption rate by B (d^{-1})	0.53	0.53	0.38	0.23	(2)
k32	*Z* export rate (d^{-1})	0.05	0.05	0.05	0.05	(3)
γ	mean algal cell S : N ratio	0.04	0.2	0.2	0.2*	(2)
I_k	saturating irradiance (W m^{-2})	5.6	7.0	11.0	15.1	(2)

* Indicates the value was derived during calibration.

† (1) Muller-Niklas and Herndl (1996); (2) Matrai and Vernet (1997); (3) Gabric et al. (1993) and references cited therein; (4) Kieber et al. (1996); (5) Hansen et al. (1996); (6) Verity et al. (1991); (7) Slagstad and Støle-Hansen (1991); (8) Billen and Becquevort (1991).

the range 0.01–0.06 d^{-1} at temperatures in the range 0–6°C.

The model formulation of bacterioplankton growth follows standard Michaelis–Menten kinetics with no temperature limitation of growth. Although bacterial biomass was measured in the Barents Sea in a contemporaneous study (Hansen et al., 1996), bacterial production rates were not measured. The studies cited above suggest that although maximum growth rates are reduced in polar waters compared with temperate regions, the mean rates appear to be similar. We have used the values of Muller-Niklas and Herndl (1996) for the reference parameter set.

3.3. *Bacterivorous nanoflagellates and large protozoa*

Hansen et al. (1996) estimated nanoflagellate grazing by assuming a typical clearance of 10^5 body volume h^{-1} and then computing ingestion as the product of clearance and bacterial biomass.

Growth was estimated assuming an efficiency (yield) factor of 0.4 (Fenchel, 1986) Microzooplankton specific growth was measured during 48-h incubations with grazing derived by assuming a growth efficiency of 0.4. Equivalent parameter values have been used in the DMS model formulation (Table 4). Hansen et al. (1996) determined biomass from cell volumes measured by microscope and by applying a carbon to volume ratio of 0.12 pg C μm^{-3} (Fenchel, 1982). Recent data from the Central Arctic (Sherr et al., 1997) suggest that herbivory by micro-heterotrophs may be more prevalent than bacterivory. If so, grazing pressure on bacteria would be reduced with a concomitant increase in bacterial turnover of DMS.

3.4. *Meso-macrozooplankton*

The larger zooplankton community was totally dominated by copepods with about 95% *Calanus* spp. (Hansen et al., 1996). Specific grazing rates (which varied from 0.01–0.18 d^{-1}) and biomass were calculated as described by Hansen et al. (1996). The biomass of copepods was much smaller than that of the microzooplankton at each station suggesting that copepod community grazing pressure was also comparatively smaller than that of the microzooplankton. Heterotrophic dinoflagellates comprised between 30–40% of zooplankton biomass at all stations.

3.5. *DMSP and DMS cycling*

DMS and its biogenic precursor DMSP are both phytoplankton metabolites. DMSP will occur both in particulate and dissolved forms and can be biodegraded by cleavage into DMS and acrylate (Kiene, 1990; Stefels and Van Boekel, 1993) or by demethylation to 3-methylmercaptopropionate (MMPA). Demethylation of MMPA produces 3-mercaptopropionate (MPA) which is catabolized with the elimination of H_2S to leave acrylate. Demethylations of DMSP to MMPA and thence to MPA are microbially mediated reactions (Taylor and Gilchrist, 1996). Methylotrophic bacteria may also consume DMS in surface waters (Kiene and Bates, 1990; Wolfe and Kiene, 1993).

The model formulation assumes that DMS and DMSP production follows first-order kinetics. Incubations experiments were done at each station at three depths within the euphotic zone to determine both net production and consumption rates (see Paper I). Net production of DMS was estimated from the rate of change in DMS sample concentration in situ. Modelled sinks for DMS include photochemical oxidation, microbial consumption and ventilation to the atmosphere.

The DMS photo-oxidation sink is scaled by the ratio of surface to average mixed layer irradiance and consequently varies diurnally and seasonally with incident solar radiation. Bacterial DMS and DMSP consumption rates were estimated from the dataset by the difference between their accumulation in untreated and chloroform-treated samples (Kiene and Bates, 1990).

The DMS and DMSP excretion rates by grazers were conservatively kept at the values used in Gabric et al. (1993). Significantly higher rates can be derived from the laboratory grazing experiments of Wolfe et al. (1994).

The ventilation of DMS to the atmosphere was calculated as the product of DMS mixed layer concentration and DMS sea-to-air transfer velocity, K_w. The transfer velocity was parameterised in terms of wind speed, w, (at 10 m) on Bjørnøya Island, (74°30′N, 19°E) and in situ ocean temperature according to Liss and Merlivat (1986), and re-scaled for DMS as given in Gabric et al. (1995),

$$\begin{aligned} K_w &= 0.17(600/\mathrm{Sc})^{2/3}w \quad \text{for } w \leqslant 3.6 \\ K_w &= (600/\mathrm{Sc})^{1/2}(2.85w - 10.26) + 0.612(600/\mathrm{Sc})^{2/3} \quad \text{for } 3.6 < w \leqslant 13 \\ K_w &= (600/\mathrm{Sc})^{1/2}(5.9w - 49.91) + 0.612(600/\mathrm{Sc})^{2/3} \quad \text{for } w > 13, \end{aligned} \tag{4}$$

where Sc is the temperature-dependent Schmidt number using the relationship given by Erikson et al. (1990).

This formulation of sea-to-air DMS transfer has been shown to be valid by Ayers et al. (1995) for waters in the Subantarctic Southern Ocean. The calculation of K_w in marginal ice zones like the Barents Sea poses special difficulties since DMS ventilation can only occur in ice-free waters. Thus, the computed DMS transfer velocity was scaled by the percentage of ice-free waters at each station as given in Table 1. Clearly this is an approximation, as it assumes a static fractional ice-cover

Table 5. *Ten most sensitive model parameters*

Parameter	Definition	Sensitivity rank
k4	Z grazing rate per organism (m^2 mg N^{-1} d^{-1})	1
k29	maximum DMS photo-oxidation rate (d^{-1})	2
k28	DMS consumption rate by B (d^{-1})	3
k23	maximum N uptake rate by P (d^{-1})	4
k11	proportion of N uptake excreted by B	5
k31	DMSP consumption rate by B (d^{-1})	6
k14	proportion of N uptake excreted by F	7
k21	DMSP excretion rate by Z (d^{-1})	8
γ	mean algal cell S : N ratio	9
k27	DMSP-DMS conversion rate (d^{-1})	10

during the bloom period and ignores other possible effects of partial ice-cover on the sea–air transfer process, e.g., the impact on effective wind fetch and the wave climate. It should also be noted that the Liss and Merlivat formulation of K_w gives about a 50% lower flux estimate compared with other formulations, e.g., Wanninkhof (1992).

3.6. *Model calibration*

Model calibration seeks to minimise the difference between the predicted and observed values of the state variables by varying the key model parameters. In our case the restricted temporal extent of the dataset precluded a proper calibration. However previous field studies (Kristiansen et al., 1994; Slagstad and Støle-Hansen, 1991) have discussed the timing and duration of the spring bloom in this region which provided a theoretical framework for comparison. The field data of Paper I were restricted to a relatively short time span at each station (compared to the duration of the spring bloom) — effectively giving only a single point in time (Table 2) albeit at four locations.

Model simulations were run for 4 months starting 1 March (Julian day 60) based on the observation that the Barents Sea spring bloom begins about mid-April (Slagstad and Støle-Hansen, 1991). Initial values for the biotic state variables were set at arbitrarily low (non-zero) values with nitrate set to 11 μM at each station, typical of late winter concentrations in the Barents Sea (Kristiansen et al., 1994; Matrai and Vernet, 1997). Because of the absence of data on sulphur species, initial DMSP and DMS pools were both set to zero.

Reference values for eighteen of the model parameters (Table 4) were derived from analysis of the Paper I data except where a parameter was not measured (e.g., bacterial production rate) in which case relevant literature values have been used. A detailed parametric sensitivity analysis of the DMS model has been carried out previously (Campolongo and Gabric, 1997) which defined the ten most sensitive parameters (Table 5). Some parameter values could vary as a result of different algal community composition at each of the sampling sites or species succession during the bloom period (Kristiansen et al., 1994) at a particular site. Consequently, a small number of the sensitive parameters were varied from their reference values during the calibration to give the best fit to the observations. These parameters are marked with an asterisk in Table 4. For example the maximum nitrate specific uptake rate, k23, would depend on the algal community composition at each sampling site as would the algal cell S : N ratio (γ) and both were varied in the calibration.

3.7. *Model uncertainty analysis*

As the model parameters are subject to measurement error, and may in some cases vary during the bloom period, it is important to quantify the error in the model predictions. The metric used to estimate uncertainty was the same as that used in the sensitivity analysis, namely, the DMS flux integrated over the 4-month bloom period. The uncertainty in this metric was estimated by a Monte-Carlo uncertainty analysis in which the model was run a large number of times for different combinations of the ten most sensitive parameters given in Table 5. This is akin to carrying out a

statistical experiment in which each model run is equivalent to a single realisation of the experiment.

Parameter set combinations were derived by randomly sampling each parameter from an assumed normal distribution with the mean as given in Table 4 and a standard deviation of 20% of the mean. A 20% error was deemed appropriate considering both analytical errors in measurement (generally less than 5%) and possible variation of the parameter over the period of the bloom. The model was run up to one thousand times with intermediate results compared until the distribution of the time-integrated DMS flux values no longer varied significantly. The results of the uncertainty analysis are given for each station in Table 6.

4. Results and discussion

The wind speed data measured by Bjørnøya Island during the study period are shown in Fig. 3. Daily mean wind speeds were high, with values above 15 ms^{-1} occurring on three occasions. The average wind speed for the entire bloom period was 7.5 ms^{-1}, with a slight decrease in the second half of the period. This is slightly higher than the long-term mean wind speed of 5.96 ms^{-1} at Bjørnøya Island during spring. DMS transfer velocity averaged 1.3 md^{-1} for the study period, similar to previously reported summer Arctic values (e.g. 1.25 md^{-1} quoted by Erikson et al. (1990) and 1.53 md^{-1} estimated by Bates et al., 1987).

Table 6. *Time-integrated DMS ventilation (mg S m^{-2}) and uncertainty (percent)*

	St I	St II	St III	St IV
flux	3.1	6.4	2.1	6.1
uncertainty	46	53	52	59

4.1. Station I

The evolution of the biotic components (P–N) during the vernal bloom is shown in Fig. 4a. The mixed layer depth is more than twice the euphotic depth at this site (Table 1) which will reduce the mean light regime available for algal photosynthesis. The high percentage ice-cover at this station affects light penetration and hence the euphotic depth and also the ventilation of DMS to the atmosphere.

The model simulation suggests that phytoplankton growth is light-limited until mid-April with a maximum standing stock of 4012 mg N m^{-2} reached at Julian Day (JD) = 144, a few days after the sampling was carried out. This is very close to the value observed during sampling of 4031 mg N m^{-2} at JD = 140. This model predicts that temporal gradients in both phytoplankton and dissolved N are very steep around the time of sampling so that large differences in these state

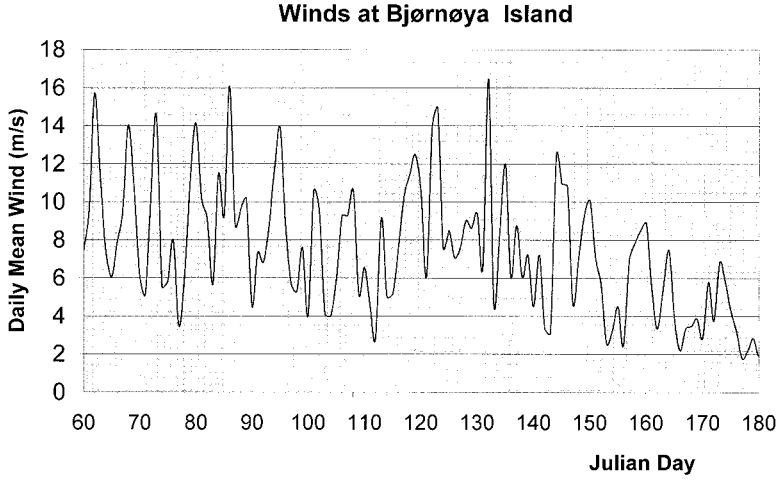

Fig. 3. Wind speeds measured at Bjørnøya Island during the study period.

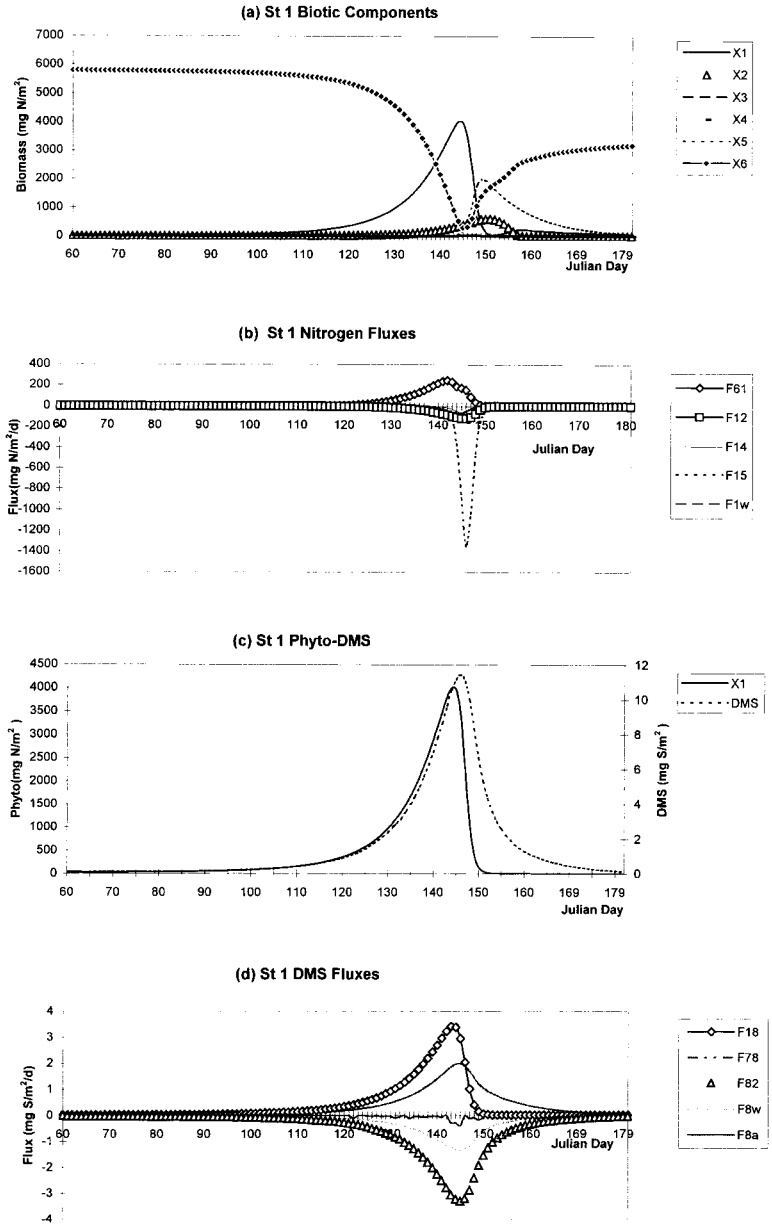

Fig. 4. Model predictions for Station I. (a) The change in biotic state variables as a function of time, (b) temporal profile of fluxes affecting the phytoplankton (P), (c) temporal correlation between the change in phytoplankton biomass and DMS, (d) temporal profile of fluxes affecting DMS (see Table 3 for explanation of codes).

variables occur over short times. DIN is predicted to drop to a value of 299 mg N m^{-2} (equivalent to 0.6 μM) at JD = 145 after which time food web regeneration increases the dissolved N (DIN) concentration. Zooplankton biomass is predicted to increase to 1983 mg N m^{-2} at JD = 149 and, by JD = 152, because of grazing, the phytoplankton are almost completely grazed down.

Nanoflagellates and large protozoa play only a minor rôle in the bloom at this station.

The temporal change in the various N fluxes that affect the phytoplankton compartment is shown in Fig. 4b. The most significant loss term for phytoplankton N at this site is grazing by meso-macrozooplankton (F_{15}).

The associated production of DMS is shown in Fig. 4c. DMS peaks at 11.4 mg S m^{-2} (corresponding to a mixed layer concentration of 9.9 nM) at JD = 146 and succeeds the phytoplankton maximum by 2 days. Importantly, DMS concentration remains at a moderate level well past the end of the phytoplankton bloom. Short time scale fluctuations in DMS concentration are due to wind speed variability and the associated change in sea-to-air flux of DMS.

The various fluxes affecting DMS turnover are shown in Fig. 4d. The strongest source of DMS was phytoplankton release (F_{18}) which peaked at 3.41 mg S m^{-2} d^{-1} around JD = 143. It is interesting to note that conversion of DMSP to DMS (F_{78}) sustains the water column DMS concentration well past the end of the phytoplankton bloom. The largest DMS sink at this site was bacterial consumption (F_{82}), which is not high enough to quickly dissipate DMS concentrations. Ventilation losses (F_{8a}) peaked at 0.41 mg S m^{-2} d^{-1} (= 13 μmoles m^{-2} d^{-1}) on JD = 145 but were comparatively small due to the 55% ice-cover at this site. The time-integrated sea-to-air DMS flux at this site over the 4-month period was 3.1 mg S m^{-2} (= 97 μmoles m^{-2}).

4.2. Station II

The result of the model simulations for Station II are shown in Fig. 5a–d. The MLD is very shallow (14 m) and about half the euphotic zone depth at this site (see Table 1) so that algal cells experience a higher average light regime than at Station I. This is reflected in the dynamics of the bloom at this site which occurs much earlier than Station I. The phytoplankton biomass reaches a peak of 1346 mg N m^{-2} at JD = 124 about 2 weeks before the time of sampling when 285 mg N m^{-2} was observed which compares well with the model prediction of 196 mg N m^{-2}. DIN is depleted with very low values from JD = 125–140, when DIN concentration would have been limiting to growth. Secondary production is low with a zooplankton peak of 24 mg N m^{-2} at JD = 143.

The temporal change in the various N fluxes that affect the phytoplankton compartment is shown in Fig. 5b. The most significant loss term for phytoplankton N is sedimentation below the thermocline (F_{1w}) due to the high algal cell sinking rate (k7) measured at this site (Table 4).

Because of the low secondary production at this site and consequently low heterotrophic excretion of DMSP, the DMS cycle (Fig. 5c) tracks the phytoplankton temporal profile very closely. The DMS peak of 4.5 mg S m^{-2} at JD = 126 (equivalent to a maximum mixed layer concentration of 10 nM) succeeds the phytoplankton maximum by 2 days. DMS concentration falls rapidly after the peak due to the reduced contribution from higher trophic levels.

The various fluxes involving DMS turnover are shown in Fig. 5d. The strongest source of DMS was again phytoplankton release which peaked at 2.3 mg S m^{-2} d^{-1} around JD = 123. Interestingly, photolysis exceeds bacterial consumption of DMS at this site. Ventilation was also a significant sink with a peak value of 1.3 mg S m^{-2} d^{-1} (= 40 μmoles m^{-2} d^{-1}) predicted on JD = 122. The time-integrated sea-to-air DMS flux at this site over the 4-month period was 6.4 mg S m^{-2} (= 199 μmoles m^{-2}).

4.3. Station III

The results of the model simulation for Station III are shown in Fig. 6a–d. This site had a significantly deeper mixed layer (65 m) than both Stations I and II. The euphotic zone depth was about half the MLD suggesting that light limitation of phytoplankton growth would be important. The model predictions support this hypothesis with the bloom onset being later in the year and peak phytoplankton biomass (2180 mg N m^{-2}) not attained until early June (JD = 154), about 10 days after sampling was carried out. Given the steep gradient the model prediction of phytoplankton biomass of 768 mg N m^{-2} compares reasonably well with observed value of 605 mg N m^{-2} on JD = 143. The predicted temporal profile of DIN, which reaches a minimum value of 6541 mg N m^{-2} (= 7.2 μM), suggests that nitrate was never limiting at this site. Secondary production is high with zooplankton biomass predicted to reach 1036 mg

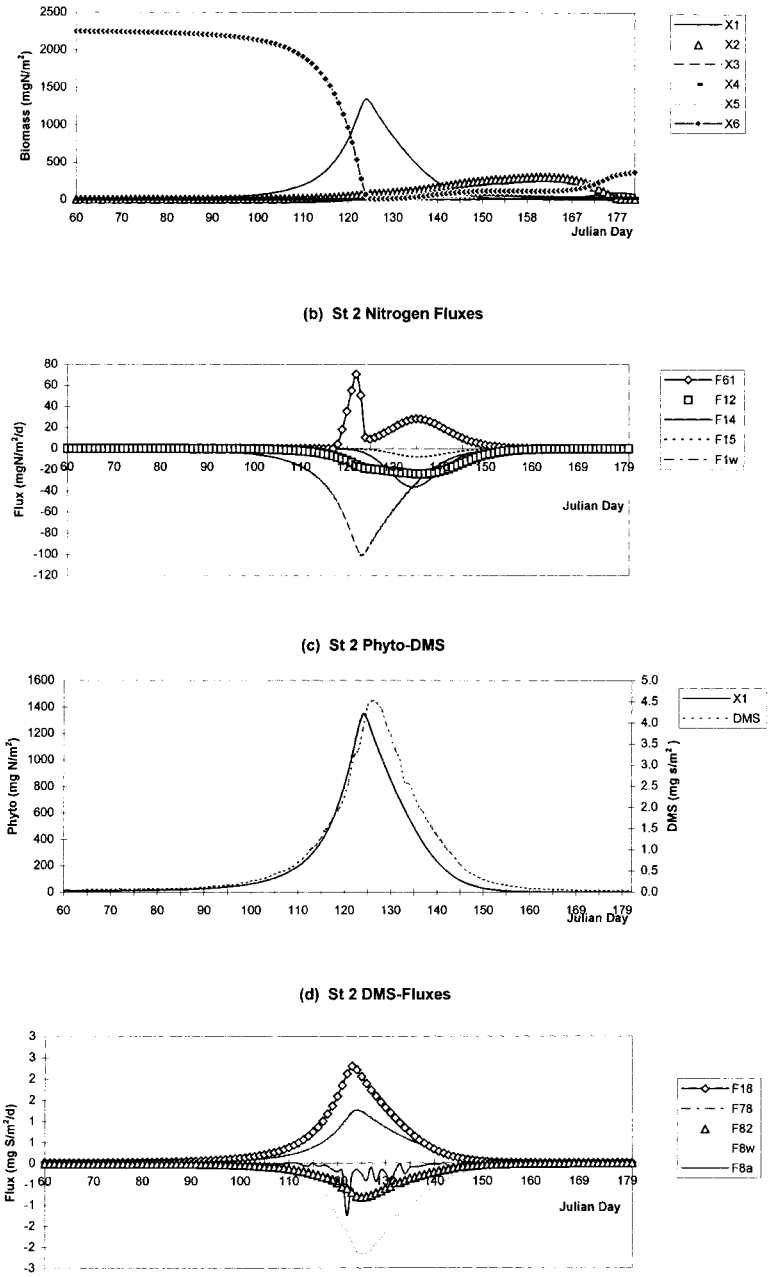

Fig. 5. Model predictions for Station II. (a) The change in biotic state variables as a function of time, (b) temporal profile of fluxes affecting the phytoplankton (P), (c) temporal correlation between the change in phytoplankton biomass and DMS, (d) temporal profile of fluxes affecting DMS (see Table 3 for explanation of codes).

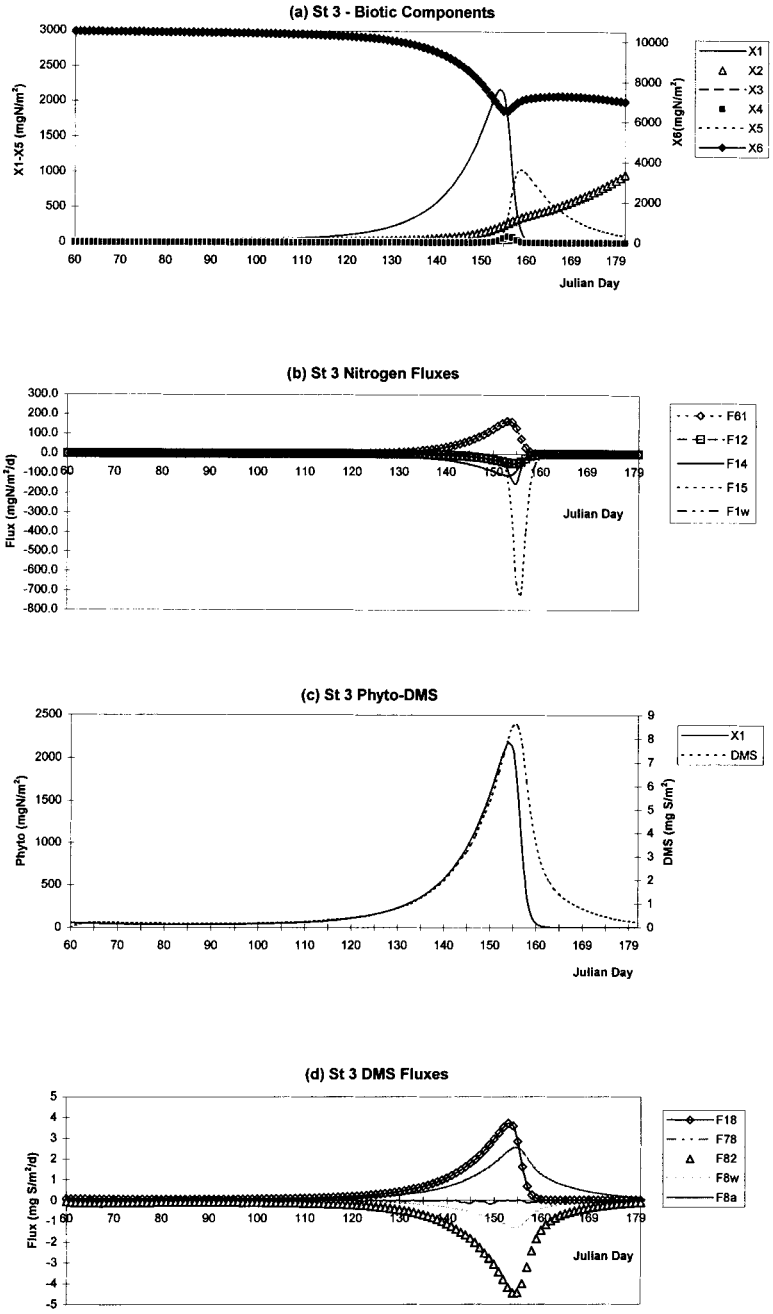

Fig. 6. Model predictions for Station III. (a) The change in biotic state variables as a function of time, (b) temporal profile of fluxes affecting the phytoplankton (P), (c) temporal correlation between the change in phytoplankton biomass and DMS, (d) temporal profile of fluxes affecting DMS (see Table 3 for explanation of codes).

N m^{-2} at JD = 159, with the phytoplankton almost completely grazed down by JD = 165.

The temporal change in the various N fluxes that affect the phytoplankton compartment is shown in Fig. 6b. The most significant loss term for phytoplankton N at this site is grazing by zooplankton.

DMS concentration is predicted to reach a peak of 8.6 mg S m^{-2} (equivalent to a mixed layer concentration 4.1 nM) at JD = 156, succeeding the phytoplankton maximum by 2 days, and remains at a significant value well past the end of the phytoplankton bloom (Fig. 6c). The predicted peak DMS value was lower than the measured value of 9.9 mg S m^{-2} at JD = 144. Although model predictions of both phytoplankton and DIN agree well with their observed values, the higher observed value of DMS (and DMSP) suggest another source at this site that was not included in the model. Advection of DMS-rich waters from the north, where the bloom occurred earlier in the season, is one possible explanation. This hypothesis is consistent with the wind direction measured at Bjørnøya Island, which was between 0–90° in the second half of May. Another possible source may result from the activity of extracellular DMSP lyase reported for *Phaeocystis* cells in temperate waters (Van den Berg et al., 1996). This prymnesiophyte represented a significant component of the phytoplankton biomass at stations II and III.

The various fluxes affecting DMS turnover are shown in Fig. 6d. The strongest source of DMS was phytoplankton release which peaked at 3.7 mg S m^{-2} d^{-1} at JD = 153 however conversion of DMSP was also significant and remained high until the end of the simulation period. The strongest DMS sink was bacterial consumption, which greatly exceeded both photolysis and ventilation. The time-integrated sea-to-air DMS flux at this site was 2.2 mg S m^{-2} (= 69 μmoles m^{-2}).

4.4. Station IV

The southernmost site had similar physico-chemical characteristics to Station III, being characterised by a deep mixed layer (61 m) but a slightly deeper euphotic zone (38 m). Model predictions (Fig. 7a) suggest that the improved light regime at this site caused an earlier bloom (cf. Station III) with peak phytoplankton biomass (2003 mg N m^{-2}) attained on JD = 140 about 5 days prior to sampling. The measured phytoplankton biomass of 985 mg N m^{-2} on JD = 145–6 compares reasonably with the model prediction of 452 mg N m^{-2}, given the very steep gradients in phytoplankton biomass predicted in the senescent stage of the bloom. Secondary production was high with zooplankton biomass reaching a peak concentration of 1054 mg N m^{-2} at JD = 146.

The temporal change in the various N fluxes that affect the phytoplankton compartment is shown in Fig. 7b. The most significant loss term for phytoplankton N at this site was grazing by micro-mesozooplankton.

DMS is predicted to lag the phytoplankton peak by 3 days and reach a peak concentration of 10.8 mg S m^{-2} (equivalent to a mixed layer concentration of 5.5 nM) (Fig. 7c), which compares very well with the observed value of 9.7 mg S m^{-2}. DMS concentration remained at a significant value well past the end of the phytoplankton bloom. The various fluxes affecting DMS turnover are shown in Fig. 7d. The strongest source of DMS was phytoplankton release which peaked at 3.4 mg S m^{-2} d^{-1} at JD = 139; however, conversion of DMSP to DMS was also high and on a time-integrated basis was actually slightly greater than phytoplankton release. The strongest DMS sink was bacterial consumption, which exceeded both photolysis and ventilation. The time-integrated sea-to-air DMS flux at this site was 6.1 mg S m^{-2} (= 193 μmoles m^{-2}).

5. Conclusions

Our aim in this modelling analysis was to fill in the temporal gaps in our knowledge of the spring bloom, which was constrained by short-term observations. The bloom timing and duration, as predicted by the model, are generally in good agreement with previous field observations in the Central Barents Sea (Sakshaug and Slagstad, 1992). During spring the bloom dynamics in this region are characterised by a complex interplay of physical and biological processes. A melt water lens observed in the Barents Sea after April, due to ice melting (Rey and Loeng, 1985), was clearly defined at Stations I (Arctic Water) and II (polar front). The strong and

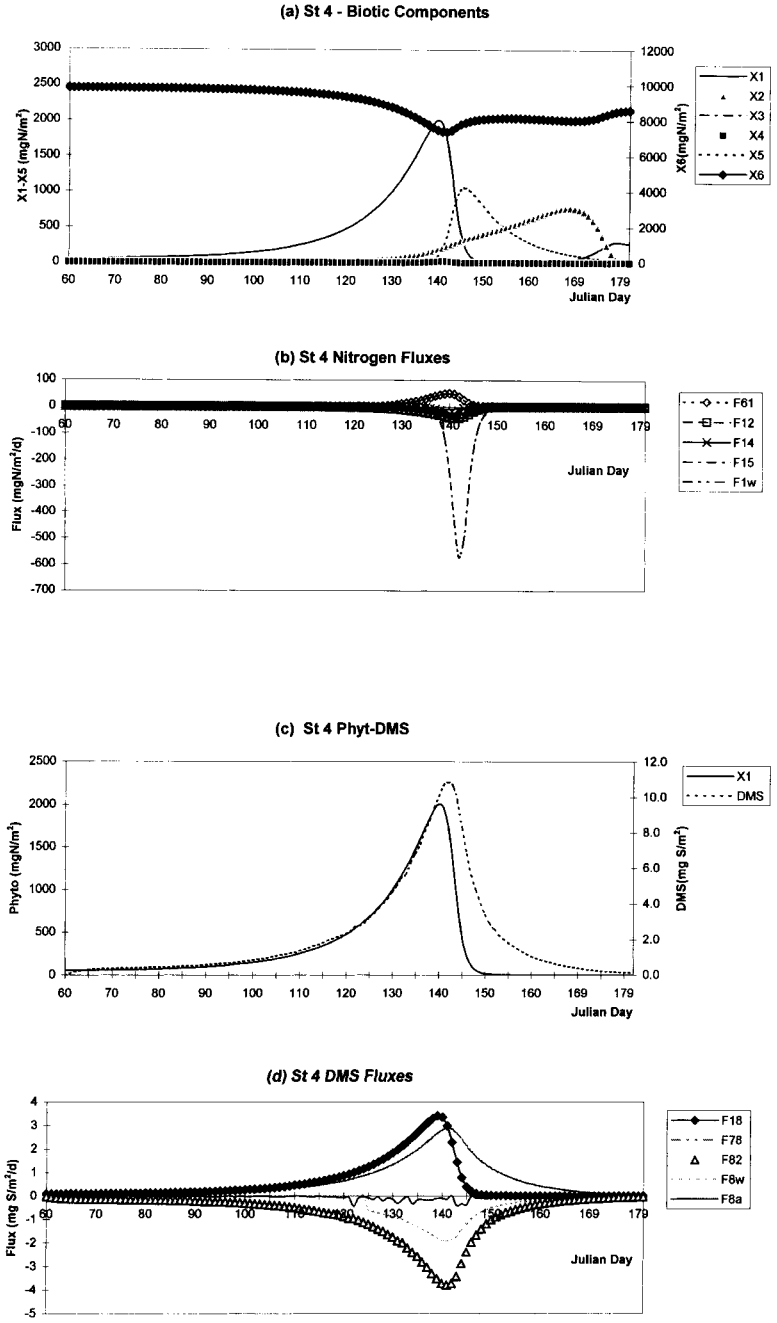

Fig. 7. Model predictions for Station IV. (a) The change in biotic state variables as a function of time, (b) temporal profile of fluxes affecting the phytoplankton (P), (c) temporal correlation between the change in phytoplankton biomass and DMS, (d) temporal profile of fluxes affecting DMS (see Table 3 for explanation of codes).

shallow halocline isolated the upper water column from deep waters exposing phytoplankton to a well-illuminated mixed layer, particularly at Station II, resulting in an early bloom at this site. In contrast, the deep thermocline in Atlantic water (at Sts. III and IV) is known to retard the onset of the spring bloom due to deep mixing of phytoplankton in spite of higher incident radiation.

The particular conditions affecting bloom development also influenced the DMS budget. For example, higher illumination at St. II, due to the strong and shallow pycnocline at the southern extension of the melt water lens, predicted DMS photolysis to be the greatest loss term, as opposed to bacterial consumption, as observed elsewhere.

The absence of melt water south of the Polar Front suggests that 1993 was not a cold year, when maximum ice extension in winter can reach Atlantic waters. Warm years are believed to retard phytoplankton blooms and promote zooplankton growth in Atlantic waters (Rey et al., 1987). The high grazing observed at Stations III and IV is in agreement with these earlier observations. Similarly, sedimentation is the main loss mechanism in the fast growing blooms in areas influenced by melt water, e.g., St. II (Sakshaug and Slagstad, 1992). High grazing at Station I, with a fast growing bloom, was not predicted from earlier observations.

Low-pressure atmospheric conditions affect the southern part of the Barents Sea with a periodicity of 10–12 days (Sakshaug and Slagstad, 1992). In the spring of 1993, the effect of wind is clearly seen in the air–sea DMS fluxes, with increasing ventilation to the atmosphere during periods of high wind. The effect of wind in ice-free waters, mainly those of Atlantic influence, is to retard and extend the period of phytoplankton growth by diluting the algal stock and injecting new nitrate from deep water into the mixed layer (Sakshaug and Slagstad, 1992). No such post-bloom dynamics were simulated in our modelling efforts as the mixed layer depth was fixed at each station and not affected by light and winds. Thus, the model is representative of the spring bloom only (April to mid-June).

The model simulations highlight a number of interacting factors that contribute to the dynamics of phytoplankton bloom and the subsequent production of DMSP and DMS. The ratio of mixed layer depth to the euphotic zone depth, R, is an important determinant of the mean light regime experienced by the algal cells, and consequently the timing of the bloom onset. Station II had the lowest value of R (see Table 1) and the earliest predicted bloom onset.

The maximum production of DMSP and DMS correlated well with the change in phytoplankton biomass, albeit with a time lag of 2–3 days. Zooplankton grazing and excretion of DMSP sustain the water column concentrations of the sulphur species well past the end of the bloom except at Station II where the influence of zooplankton biomass and grazing was lessened due to the high particulate sedimentation rate. The model predictions reinforce the hypothesis of Paper I that algal taxonomy is not the most important determinant of DMS concentrations in these waters. Indeed a maximum DMS concentration of 9.9 nM was predicted at Station I, although the phytoplankton community was diatom dominated at this site.

In waters of high biological productivity such as Arctic shelves (e.g., the Barents Sea), surface ocean DMS concentration may be underestimated by areal averages such as those of Bates et al. (1987) and Erickson et al. (1990) due to a paucity of measurements. This study has highlighted the importance of temporal and spatial variations and the need for longer term sampling programmes. An average of 1.4 nM was reported by Bates above for spring–summer in the north Pacific while a range of 7.8–25 nM was reported for the Barents Sea during the spring bloom (Paper I) and a range of 5.5–10 nM in the Greenland Sea during late summer (Leck and Persson, 1996).

Although ventilation was the smallest DMS sink at each site, except at Station II, the time-integrated sea-to-air flux was nevertheless significant with a mean over all stations of 4.4 mg S m^{-2}. The model predicts that the peak DMS ventilation pulse could be as high as 1.3 mg S m^{-2} d^{-1}, the maximum daily value simulated at Station II. This is almost double the peak value of 0.7 mg S m^{-2} d^{-1} calculated by Levasseur et al. (1994) in the Arctic Ocean off Greenland during April–May. Taking the mean of all stations over the simulated active growth period ($\cong$ 70 days) the resulting average daily flux for the Barents Sea was 0.063 mg S m^{-2} d^{-1}. Given the uncertainty in our estimates, this is in agreement with the area average estimates of Bates et al. (1987) (0.067 mg S m^{-2} d^{-1}) and Leck and Persson (1996) (0.064 mg S m^{-2} d^{-1}) and that of Erickson

et al. (1990) (0.10 mg S m^{-2} d^{-1}) for Arctic waters during summer.

The model indicates that the ventilation flux is very variable in time so that a seasonal budget estimate based on a short period of observations might well be biased. On the other hand, DMS loss due to biological fluxes, such as bacterial consumption, displays a smoother temporal profile. These observations, coupled with the sharp temporal gradient predicted by the model for the phytoplankton, strongly point to the need to sample the system's dynamics over a longer cycle, including prior to and through the bloom evolution. This is especially important in areas where changing ice coverage can result in significant variation in biological productivity, as has been shown to occur in the Barents Sea (Slagstad and Wassmann, 1998).

6. Acknowledgments

The Bjørnøya Island meteorological data were kindly provided by Dag Slagstad. The modelling component of this work was partially supported by the Australian Research Council Small Research Grant Scheme and the Griffith University National Competitive Grants Support Scheme. The first author gratefully acknowledges the hospitality of Scripps Institution of Oceanography, La Jolla, California during November–December 1997. This project was also funded by grants from the National Science Foundation (OPP-92-00847, OPP-97–4723 (P. A. Matrai) and OPP-92-00436, OPP-97-09779 (M. Vernet).

REFERENCES

Andersen, P. 1988. The quantitative importance of the "microbial loop" in the marine pelagic: a case study from the North Bering/Chukchi Sea. *Arch. Hydrobiol.* **31**, 243–251.

Ayers, G. P., Gillet, R. W, Ivey, J. P., Schafer, B. and Gabric, A. J. 1995. Short-term variability in marine atmospheric dimethylsulphide concentration. *Geophys. Res. Lett.* **22**, 18, 2513–2516.

Azam, F., Fenchel, T., Gray, J. S., Meyer-Reil, L. A. and Thingstad, F. 1983. The ecological role of water-column microbes in the sea. *Mar. Ecol. Prog. Ser.* **10**, 257–263.

Barnard, W. R., Andreae, M. O. and Iverson, R. L. 1984. Dimethylsulphide and *Phaeocycstis pouchetti* in the southeastern Bering Sea. *Cont. Shelf Res.* **3**, 103–113.

Bates, T. S., Cline, J. D., Gammon, R. H. and Kelly-Hansen, S. R. 1987. Regional and seasonal variations in the flux of oceanic dimethylsulphide to the atmosphere. *J. Geophys. Res.* **92**, C3, 2930–2938.

Bates, T. S., Lamb, B. K., Guenther, A., Dignon, J. and Stoiber, R. E. 1992. Sulfur emissions to the atmosphere from natural sources. *J. Atmos. Chem.* **14**, 315–337.

Billen, G. and Becquevort, S. 1991. Phytoplankton-bacteria relationships in the Antarctic marine ecosystem. *Polar Res.* **10**, 245–253.

Brock, T. D. 1981. Calculating solar radiation for ecological studies. *Ecol. Model.* **14**, 1–19.

Bunt, J. S. and Lee, C. C. 1970. Seasonal primary production in Antarctic sea ice at McMurdo Sound in 1967. *J. Mar. Res.* **28**, 304–320.

Campolongo, F. and Gabric, A. J. 1997. The parametric sensitivity of dimethylsulphide flux in the Southern Ocean. *J. Stat. Comp. and Sim.* **57**, 337–352.

Charlson, R. J., Lovelock, J. E., Andreae, M. O. and Warren, S. G. 1987. Oceanic phytoplankton, atmospheric sulphur, cloud albedo and climate. *Nature* **326**, 655–661.

Eppley, R. W. 1972. Temperature and phytoplankton growth in the sea. *Fish. Bull.* **70**, 1063–1085.

Erickson, D. J., Ghan, S. J. and Penner, J. E. 1990. Global ocean-to-atmosphere dimethylsulfide flux. *J. Geophys. Res.* **95**, D6, 7543–7552.

Fenchel, T. 1982. Ecology of heterotrophic microflagellates. IV. Quantitative occurrence and importance as bacterial consumers. *Mar. Ecol. Prog. Ser.* **9**, 35–42.

Fenchel, T. 1986. Protozoan filter feeding. *Prog. Protistol.* **1**, 63–113.

Fenchel, T. 1988. Marine plankton food chains. *Ann. Rev. Ecol. Syst.* **19**, 19–38.

Gabric, A. J., Murray, C. N., Stone, L. and Kohl, M. 1993. Modelling the production of dimethylsulphide during a phytoplankton bloom. *J. Geophys. Res.* **98**, C12, 22805–22816.

Gabric, A. J., Ayers, G. P. and Sander, G. C. 1995. Independent marine and atmospheric model estimates of the sea–air flux of dimethylsulphide in the Southern Ocean. *Geophys. Res. Lett.* **22**, 24, 3521–3524.

Gabric, A. J., Ayers, G. P., Murray C. N. and Parslow, J. 1996. Use of remote sensing and mathematical modelling to predict the flux of dimethylsulphide to the atmosphere in the Southern Ocean. *Adv. in Space Res.* **18**, 7, 117–128.

Gabric, A. J., Whetton, P. H., Boers, R. and Ayers, G. P. 1998. The impact of simulated climate change on the air–sea flux of dimethylsulphide in the Subantarctic Southern Ocean. *Tellus* **50B**, 388–399.

Gibson, J. A. E., Garrick, R. C., Burton, H. R. and McTaggart, A. R. 1990. Dimethylsulphide and the alga

Phaeocystis pouchetti in antarctic coastal waters. *Mar. Biol.* **104**, 339–346.

Groene, T. 1995. Biogenic production and consumption of DMS and DMSP in the marine epipelagic zone: a review. *J. Mar. Systems* **6**, 191–209.

Hansen, B., Christiansen, S. and Pedersen, G. 1996. Plankton dynamics in the marginal ice zone of the central Barents Sea during spring: Carbon flow and structure of the grazer food chain. *Polar. Biol.* **16**, 115–128.

Heintzenberg, J. and Leck, C. 1994. Seasonal variation of the atmospheric aerosol near the top of the marine boundary layer over Spitsbergen related to the Arctic sulphur cycle. *Tellus* **46B**, 52–67.

Keller, M. D., Bellows, W. K. and Guillard, R. L. 1989. Dimethyl sulfide production in marine phytoplankton. In: *Biogenic sulfur in the environment* (eds. Saltzman, E.S. and Cooper, W. J.). American Chemical Society, Washington, D.C.

Kieber, D. J., Jiao, J., Kiene, R. P. and Bates, T. S. 1996. Impact of dimethyl sulfide photochemistry on methyl sulfur cycling in the equatorial Pacific. *J. Geophys. Res.* **101**, 3715–3722.

Kiene, R. P. 1990. Dimethyl sulfide production from dimethyl sulfoniopropionate in coastal seawater samples and bacterial cultures. *Appl. Environ. Microbiol.* **56**, 3292–3297.

Kiene, R. P. and Bates, T. S. 1990. Biological removal of dimethylsulphide from seawater. *Nature* **345**, 702–705.

Kirst, G. O., Thiel, C., Wolff, H., Nothnagel, J., Wanzek, M. and Ulmke, R. 1991. Dimethylsulfoniopropionate (DMSP) in ice algae and its possible biological role. *Mar. Chem.* **35**, 381–388.

Kristiansen, S., Farbrot, T. and Wheeler, P. A. 1994. Nitrogen cycling in the Barents Sea — Seasonal dynamics of new and regenerated production in the marginal ice zone. *Limnol. Oceanogr.* **39**, 1630–1642.

Leck, C. and Persson, C. 1996 The central Arctic Ocean as a source of dimethyl sulfide. Seasonal variability in relation to biological activity. *Tellus* **48B**, 156–177.

Levasseur, M., Gosselin, M. and Michaud, S. 1994. A new source of dimethyl sulfide for the Arctic atmosphere. *Mar. Biol.* **121**, 381–387.

Li, S.-M., Barrie, L. A. and Sirois, A. 1993. Biogenic sulfur aerosol in the Arctic troposphere: II. Trends and seasonal variations. *J. Geophys. Res.* **98**, 20623–20631.

Liss, P. S. and Merlivat, L. 1986. Air–sea gas exchange rates: Introduction and synthesis. In: *The rôle of air–sea exchange in geochemical cycling* (ed. (Buat-Menard, P.), pp. 113–127. Reidel, Hingham, MA.

Liss, P. S., Malin, G., Turner, S. M., Holligan, P. M. 1994. Dimethylsulphide and *Phaeocystis*. A review. *J. Mar. Sys.* **5**, 41–53.

Loeng, H. 1991. Features of the physical oceanographic conditions of the Barents Sea. *Polar Res.* **10**, 5–18.

Matrai, P. A. and Vernet, M. 1997. Dynamics of the vernal bloom in the marginal ice-zone of the Barents Sea: Dimethyl sulfide and dimethylsulfoniopropionate budgets. *J. Geophys Res.* **102**, 22965–22979.

McTaggart, A. R. and Burton, H. 1992. Dimethyl sulfide concentrations in the surface waters of the Australian Antarctic and subantarctic oceans during an austral summer. *J. Geophys. Res.* **97** (C9), 14407–14412.

Meszaros, E. 1988. On the possible role of the biosphere in the control of atmospheric clouds and precipitation. *Atmos. Environ.* **22**, 423–424.

Muller-Niklas, G. and Herndl, G. J. 1996. Dynamics of bacterioplankton during a phytoplankton bloom in the high Arctic waters of the Franz-Joseph Land archipelago. *Aquat. Microb. Ecol.* **11**, 111–118.

Nagata, T. 1986. Carbon and nitrogen content of natural planktonic bacteria. *Appl. Environ. Microbiol.* **52**, 28–32.

Neori, A. and Holm-Hansen, O. 1982. Effect of temperature on rate of photosynthesis in Antarctic phytoplankton. *Polar Biology* **1**, 33–38.

Nielsen, T. G. and Hansen, B. 1995. Plankton community structure and carbon cycling on the western coast of Greenland during and after the sedimentation of a diatom bloom. *Mar. Ecol. Prog. Ser.* **125**, 239–257.

Platt, T., Denman, K. L. and Jassby, A. D. 1977. Modeling the productivity of phytoplankton. In: *The sea*, vol. 6 (ed. Goldberg, E. D.). New York, Wiley, pp. 807–856.

Pomeroy, L. R. and Diebel, D. 1986. Temperature regulation of bacterial activity during the spring bloom in Newfoundland coastal waters. *Science* **233**, 359–361.

Rey, F. 1991. Photosynthesis-irradiance relationships in natural phytoplankton populations of the Barents Sea. *Polar Res.* **10**, 105–116.

Rey, F. and Loeng, H. 1985. The influence of ice and hydrographic conditions on the development of phytoplankton in the Barents Sea. In: *The marine biology of polar regions and effects of stress on marine organisms* (eds. Gray, J. S. and Christiansen, M. E.). New York, John Wiley, pp. 49–63.

Rey, F., Skjoldal, H. R. and Slagstad, D. 1987. Primary production in relation to climatic changes in the Barents Sea. In: *The effect of oceanographic conditions on distribution and population dynamics of commercial fish stocks in the Barents Sea*. Proc. 3rd Soviet–Norwegian Symposium (ed. Loeng, H.), pp. 29–46. Inst. of Mar. Res., Bergen, Norway.

Rich, J., Kirchman, D. L., Gosselin, M., Sherr, E and Sherr, B. 1997. High bacterial production, uptake and concentrations of dissolved organic matter in the Central Arctic Ocean. *Deep-Sea Res. II* **44**, 1645–1664.

Rivkin, R. B., Anderson, M. R. and Lajzerowicz, C. 1996. Microbial processes in cold oceans. I. Relationship between temperature and bacterial growth rate. *Aquat. Microb. Ecol.* **10**, 243–254.

Sakshaug, E. and Slagstad, S. 1992. Sea ice and wind: effects on primary productivity in the Barents Sea. *Atmosphere-Ocean.* **30**, 579–591.

Shaw, G. E. 1987. Aerosols as climate regulators: a climate biosphere linkage? *Atmos. Environ.* **21**, 985–986.

Sherr, E. B., Sherr, B. F. and Fessenden, L. 1997. Heterotrophic protists in the Central Arctic Ocean. *Deep-Sea Res. II* **48**, 1665–1682.

Slagstad, D. and Støle-Hansen, K. 1991. Dynamics of plankton growth in the Barents Sea. *Polar Res.* **10**, 173–186.

Smith, E. L. 1936. Photosynthesis in relation to light and carbon dioxide. *Proc. Nat. Acad. Science* **22**, 504–511.

Stefels, J. and Van Boekel, W. H. M. 1993. Production of DMS from dissolved DMSP in axenic cultures of the marine phytoplankton species *P. pouchetii*. *Mar. Ecol. Prog. Ser.* **97**, 11–18.

Strickland, J. D. H. 1960. Measuring the production of marine phytoplankton. *Bull. Fish. Res. Board Can.* **122**, 1–172.

Talling, J. F. 1957. Photosynthetic characteristics of some freshwater plankton diatoms in relation to underwater radiation. *New Phytol.* **56**, 29–50.

Taylor, B. F. and Gilchrist, P. T. 1996. Metabolic pathways involved in DMSP degradation. In: *Biological environmental chemistry of DMSP and related sulfonium compounds* (eds. Kiene, R. P., Visscher, P. T., Keller, M. D. and Kirst, G. O.). Plenum Press, New York, pp. 265–276.

Thingstad, F. and Martinussen, I. 1991. Are bacteria active in the cold pelagic ecosystem of the Barents Sea? *Polar. Res.* **10**, 255–266.

Verity, P. G., Smayda, T. J. and Sakshaug, E. 1991. Photosynthesis, excretion, and growth of Phaeocystis colonies and solitary cells. *Polar. Res.* **10**, 117–128.

Vernet, M., Matrai, P. A. and Andreassen, I. 1998. Synthesis of particulate and extracellular carbon by phytoplankton in the Barents Sea. *J. Geophys. Res.* **102**, 1023–1037.

Wanninkhof, R. 1992. Relationship between gas exchange and wind speed over the ocean. *J. Geophys. Res.* **97**, 7373–7382.

Wassmann, P., Vernet, M., Mitchell, B. G. and Rey, F. 1990. Mass sedimentation of *Phaeocystis pouchetti* in the Barents Sea. *Mar. Ecol. Prog. Ser.* **66**, 183–195.

Wassmann, P., Ratkova, T. N., Andreassen, I., Vernet, M., Pedersen, G. and Rey, F. 1999. Spring bloom development in the marginal ice zone and the Central Barents Sea. *P.S.Z.N.I.: Marine Ecology*, in press.

Wolfe, G. V. and Kiene, R. P. 1993. Radioisotope and chemical inhibitor measurements of dimethyl sulfide consumption rates and kinetics in estuarine waters. *Mar. Ecol. Prog. Ser.* **99**, 261–269.

Wolfe, G. V., Sherr, E. B. and Sherr, B. F. 1994. Release and consumption of DMSP from *Emiliana huxleyi* during grazing by *Oxyrrhis marina*. *Mar. Ecol. Progr. Ser.* **111**, 111–119.